JOURNAL OF PROPULSION AND POWER
Vol. 11, No. 3, May–June 1995

Performance Variation of Scramjet Nozzle at Various Nozzle Pressure Ratios

Tetsuo Hiraiwa,* Sadatake Tomioka,* Shuuichi Ueda,† and Tohru Mitani‡
National Aerospace Laboratory, Kakuda Research Center, Kakuda, Miyagi 981-15, Japan
and
Masahiko Yamamoto§ and Masashi Matsumoto¶
Ishikawajima–Harima Heavy Industries, Chiyoda-ku, Tokyo 100, Japan

An experimental study of scramjet nozzle was conducted to investigate how the nozzle flow is affected by ambient pressure. In order to elucidate the aerodynamic properties of nozzle flow, detailed measurements of thrust and wall pressure were carried out using cold nitrogen. Nozzle flow was also visualized using a shear sensitive liquid crystal. Wall pressure and shear stress distributions in an overexpanded nozzle showed that nozzle flow includes a crossing shock wave made at the side-fences. This flowfield can be approximated as a supersonic inlet flow compressed by sidewalls. The high-pressure region on the nozzle ramp generated by the shock waves results in a higher performance in scramjet nozzle than that estimated for a two-dimensional separation from the ramp.

Nomenclature

C_F = thrust coefficient
EN5 = external nozzle with the expansion ratio, ε of 5
P, Ps = static pressure on nozzle walls
Pc = total pressure of nozzle flow
Pv = ambient pressure
S = surface area
Tc = total temperature of nozzle flow
Y^* = half-height of the gas generator throat, 4 mm
ϑ = inclination angle of ramp, 15 deg

Subscripts
e = experimental
i = nozzle inlet
r = ramp
s = separation point

I. Introduction

HYPERSONIC airbreathing vehicles, such as the National Aero-Space Plane (NASP), require efficient airframe propulsion integration.[1] The propulsion system of NASP will be based on the scramjet system during a major portion of its mission. In this system, the nozzle is designed as a single expansion ramp nozzle (SERN) to minimize friction drag and nozzle weight while extracting thrust from the high-pressure flow on the aftbody.[2,3] As the nozzle generates the major portion of thrust, the performance of the nozzle dominates the thrust efficiency of the whole propulsion system. Thus, accurate estimation and prediction of nozzle performance is essential in the development of scramjet engines. Furthermore, hypersonic vehicles experience large variations in ambient or "back" pressure in flight. The change in back pressure can significantly alter the thrust and pitching moment generated in the nozzle, especially when the nozzle's internal flow is affected by external conditions. Thus, investigation of nozzle performance in off-design conditions is important for estimation of the feasibility of SERN for hypersonic vehicles.

Both experimental and numerical studies on SERNs have been carried out to investigate the interaction between the nozzle internal flow and the external conditions. Simulated flight conditions in these studies have recently been extended to the hypersonic regime. Ruffin et al.[4] calculated the flowfield in SERN in an underexpanded condition with an implicit Navier-Stokes solver and compared the results with experimental data. Watanabe[5] investigated the flowfield in SERN in both underexpanded and overexpanded conditions experimentally. He also examined the effect of side-fence shapes on the flowfield. Zeutzius and Beylich[6] conducted an experimental investigation on the effects of parameters such as aspect ratio and scarf angle on the flowfield in a scarfed SERN. These studies, however, concentrated on the investigation of the flowfield in SERNs, while the effect of the interaction, namely the separation, on SERN performance remains uninvestigated.

The objective of the present study is to investigate the variation of nozzle performance with the change in external conditions. A scarfed nozzle[6] was selected to minimize the three dimensionality of the flow on the nozzle ramp. The effect of ambient pressure was measured in terms of nozzle pressure ratio (NPR), defined as the ratio of the nozzle total pressure to the ambient pressure. Total pressure of the nozzle flow was varied to change the NPR. Thrust delivered by a scramjet nozzle was measured in both underexpanded and overexpanded conditions. Obtained thrust efficiency was compared with predicted values. A simple prediction method based on the assumption that flowfield is two dimensional was adopted to predict the variation of nozzle performance. In the overexpanded condition, the treatment of interference of the internal flow with the external flow, viz., the separation of flow, becomes very important in the prediction of the nozzle performance. In the present study, two-dimensional separation was assumed. The flowfield in the nozzle in the overexpanded condition was observed to investigate the nature of the interference between the nozzle internal flow and the external conditions.

Received June 15, 1992; revision received Feb. 19, 1994; accepted for publication Feb. 25, 1994.

*Researcher, Ramjet Combustion Laboratory.
†Researcher, Rocket Altitude Performance Laboratory.
‡Head, Ramjet Combustion Laboratory. Member AIAA.
§Engineer, Engine Design Department, Research and Engineering Division, Aero-Engine and Space Operations (Tanashi).
¶Research Engineer, Fluid Dynamics and Combustion Department, Research Institute (Toyosu).

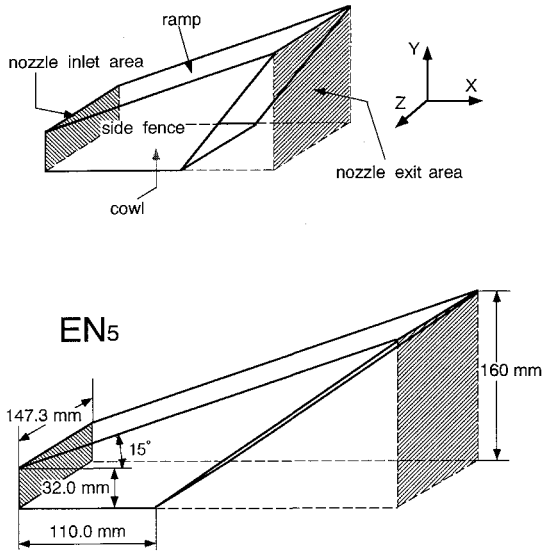

Fig. 1 Schematic of the scramjet nozzle, external nozzle with expansion ratio of 5 (EN5).

II. Experimental Methods

A. Scramjet Nozzle

A schematic of the nozzle, called EN5, is presented in Fig. 1. This nozzle is a kind of SERN with plane walls, a ramp, a cowl, and side-fences. The ramp, corresponding to the underbelly of the airframe, is a flat plate inclined to the X axis by 15 deg. The cowl and side-fences are parallel to the X axis. The length of the ramp and that of the cowl were chosen to optimize the flowfield of the nozzle, unless the wave emerging from the trailing edge of the cowl interacted with the ramp.[7]

The expansion ratio ε is defined as the ratio of a nozzle exit area to a nozzle entrance area, indicated by the shading in Fig. 1. The nozzle exit area is a projected area on a plane and perpendicular to the X axis at the trailing edge of the ramp. The ratio of 5 corresponds to the ratio of an optimum nozzle indicated by Snyder and Pinckney.[2] The cross section of the nozzle inlet is a rectangle, 147.3 × 32 mm.

Shear stress sensitive liquid crystal [(SSLC); Merck Industrial Chemicals; TI511] was used to visualize the nozzle flowfield on the ramp and the side-fence. Liquid crystal was painted over the blackened area under investigation. The liquid crystal is highly sensitive to shear stress, but nearly independent of temperature. The color of the crystal changes from red to blue in order of the spectrum as the surface shear stress increases. The variation of color was recorded by charge-coupled device (CCD) and conventional cameras.

The oil point method was used to visualize flow directions on the nozzle walls. In this study, the ramp wall was dotted with over 1000 points and was observed in several conditions in the region NPR < 100. The shadowgraph method was also used to visualize the flow in the nozzles. The wall pressures Ps were measured at 150 wall pressure taps in EN5 using three scanning pressure sensors. Details can be found in Ref. 8.

B. Testing Configuration

All the experiments were carried out under subatmospheric conditions in a high-altitude test stand (HATS) at the National Aerospace Laboratory, Kakuda Research Center. This HATS can simulate ambient pressure less than 10 hPa, for 180 s. Figure 2 shows the configuration of the test apparatus in the test cell of HATS. The scramjet nozzle was connected with a gas generator (GG) installed on a thrust measuring system (TMS). The thrust was measured by load cells on the TMS and compared with the values obtained by integrating the static pressures in the nozzles.

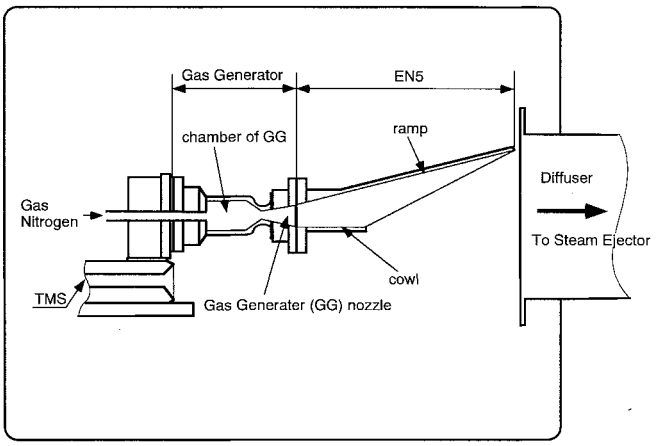

Fig. 2 Experimental apparatus in the test cell of High Altitude Test Stand at National Aerospace Laboratory—Kakuda Research Center.

The GG was used to simulate the exhaust flow from the scramjet combustor. The nozzle of the GG was designed to be wave-free for the hot combustion flow generated by monomethyl-hydrazine/nitrogen tetraoxide (MMH/NTO). Therefore, the nozzle of the GG created a pair of compression waves. The experiments were conducted with a nozzle flow with a total temperature Tc of 293 K, and a total pressure Pc of 1.0 MPa. The cross section of the GG throat was a rectangle, 147.3 × 8 mm, and the expansion ratio ε of the GG nozzle was 4. The GG nozzle accelerated the cold flow to Mach 2.9 at the exit of the GG.

C. Off-Design Performance Test

The effects of ambient pressure on the nozzles were investigated at varying NPR. In most previous experiments Pv has been controlled to change the NPR.[9,10] In this study, however, NPR was changed continuously by controlling the total pressure of the nozzle exhaust flow, rather than by controlling ambient pressure. The unit Reynolds number of the flow was evaluated to be 2.1 × 10^7/m under the nominal condition of Pc = 1.0 MPa. The Reynolds number was not constant in the off-design performance tests. Preliminary experiments indicated that the flow in the scramjet nozzles was turbulent and that the variation of Pc did not alter the features of flow significantly.[8]

The nozzle performance influenced by Pv was measured in terms of C_F. C_F is the ratio of the experimental Isp to the ideal Isp of the nozzle. The ideal Isp for a given NPR was estimated by a one-dimensional isentropic calculation. The measured mass flow rate of N_2 was corrected in consideration of the real gas effect and the delay in discharge rates in the supply system. Hysteresis in C_F variation with NPR was observed at lower NPR. When NPR was decreased, the flow separated from the ramp completely at NPR = 18. When NPR was increased, the separated flow reattached to the ramp at NPR = 25. At NPR > 25, there was no difference between the C_F variations measured when NPR was decreased and increased.

The thrust coefficient is a function of thrust, total pressure, temperature, and flow rate. Thrust is measured with the uncertainty of ±0.1%. The uncertainties of pressure and temperature were ±1%, and that of turbine flow meter was ±0.5%. The maximum uncertainties of measured C_F were estimated as ±1.7% at NPR = 200 and ±2.3% at NPR = 30.

D. Prediction of the Thrust Coefficient Variation

The variation of the thrust coefficient can be predicted utilizing thrust in a vacuum, calculated with improved TDK code.[8] This code was used to estimate the performance of EN5 and wall pressure distributions in a vacuum. It is assumed

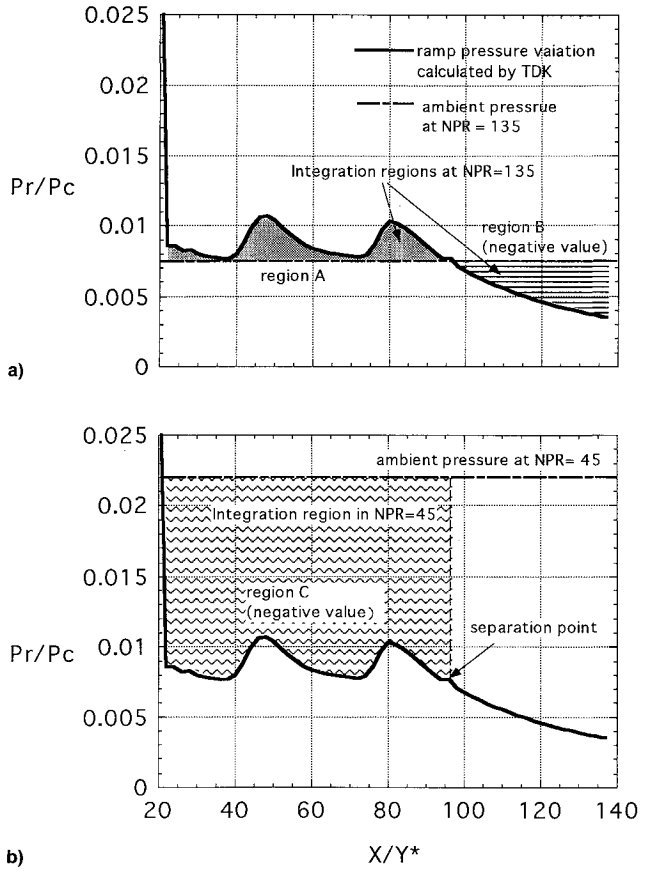

Fig. 3 Integration regions of EN5 nozzle wall pressure on the ramp at NPR = a) 135 and b) 45.

in this method that the flow in the nozzle is two dimensional and that separation occurs two dimensionally.

The C_F in the underexpanded condition can be estimated by subtraction of the drag produced by Pv from the calculated thrust in a vacuum:

$$C_{F,\text{under,EN5}},\ C_{F,\text{GG}} = \left[(Isp_{,\text{vacuum,TDK}} - \frac{\varepsilon C^*}{\text{NPR}} - \text{FL})/Vei \right] \quad (1)$$

C^* is the characteristic velocity and Vei is the nozzle exhaust velocity when the expansion is isentropic. The friction loss (FL) was 6.3 kg/s in the GG nozzle and 4.2 kg/s in EN5.[8]

The C_F variation in the overexpanded condition can be calculated with a integration of wall pressure on the ramp. Figure 3 shows the pressure distributions and integration regions at NPR = 45 and 135.

At NPR = 135, the flow did not separate from the ramp. Nominal thrust of the ramp can be estimated by integrating the nominal pressure in region A (positive thrust) and B (negative thrust) as shown in Fig. 3. It is assumed that the separation occurs at the point where a local wall pressure is smaller than one-third of the ambient pressure.[11] For example, the nominal Isp (negative value) at NPR = 45 can be given by integrating the pressure in region C of Fig. 3. It can be estimated that the ramp flow at the trailing edge begins to separate at NPR = 94, and the flow separates completely from the ramp at NPR = 30.

The Isp of overexpanded EN5 is given by Eq. (2):

$$Isp_{,\text{ramp,TDK}} = \left[\int_{X_{ri}}^{X_{rs}} (P_{r,\text{TDK}} - Pv)\Delta S \sin \upsilon \frac{dx}{\dot{m}} \right] \quad (2)$$

The C_F of EN5 in the overexpanded condition is determined from Eqs. (1) and (2):

$$C_{F,\text{over}} = C_{F,\text{GG}} + [(Isp_{,\text{ramp,TDK}_{\text{EN5}}} - \text{FL}_{\text{EN5}})/Vei] \quad (3)$$

The friction loss in EN5 decreases as the wet area in the nozzle decreases. However, it is difficult to estimate the FL when the separation occurs. The FL in EN5 corresponds to approximately 1% in C_F. Therefore, in Eq. (3) it is assumed that the FL has a constant value that is the same as that in underexpansion. The predicted C_F does not qualitatively differ from the C_F variation when the FL is estimated correctly.

III. Results and Discussion

A. Experimental Results of the Thrust Coefficient

Performances of the nozzles are shown in Fig. 4. Experimental results, shown as open circles, are presented at NPR = 1000 to 10. These results were measured when NPR was decreased. The predicted C_F of the EN and the GG nozzles are shown as a solid line and a broken line, respectively.

An optimum expansion of SERN is defined as a condition where the ambient pressure is equal to the static pressure at the trailing edge of the nozzle. The NPR in the optimum condition of EN5, which is estimated from the data calculated using the TDK code, is 284. Figure 4 shows, however, that the peak C_F of EN5 is observed at NPR = 380.

At NPR < 380, C_F of the overexpanded EN5 drops off as the NPR is increased. The predicted values of C_F agree with the experimental results within −1.0% in this condition. The predicted C_F at NPR = 100–200 also agrees with the experimental results within the same order of error as that in the underexpanded condition.

Under the condition of NPR < 100, the experimental C_F is lower than the predicted C_F of GG. This result indicated that the EN5 nozzle generated loss to the total thrust of the scramjet system, e.g., about 14% at NPR = 20.

Comparing the predicted C_F of EN5 with the prediction, no agreement can be found between the prediction and the experimental results. The experimental C_F does not decrease monotonously as NPR is decreased. A slight plateau was observed in the experimental C_F at NPR = 55–90. Using shadowgraph visualization, it was found that flow separated from the ramp completely at NPR = 18. In contrast, the predicted C_F displayed a monotonous decrease to NPR = 31, at which point the flow separated completely from the ramp.

C_F cannot be interpreted on the assumption that the flow is two dimensional in the overexpanded nozzle. In order to determine the reasons for disagreement with the prediction, the flowfield in the overexpanded EN5 nozzle was investigated as discussed in the following sections.

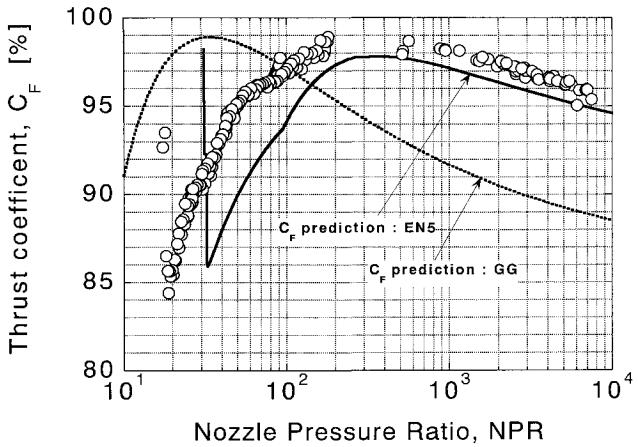

Fig. 4 Comparison of experimental thrust coefficients and predicted results.

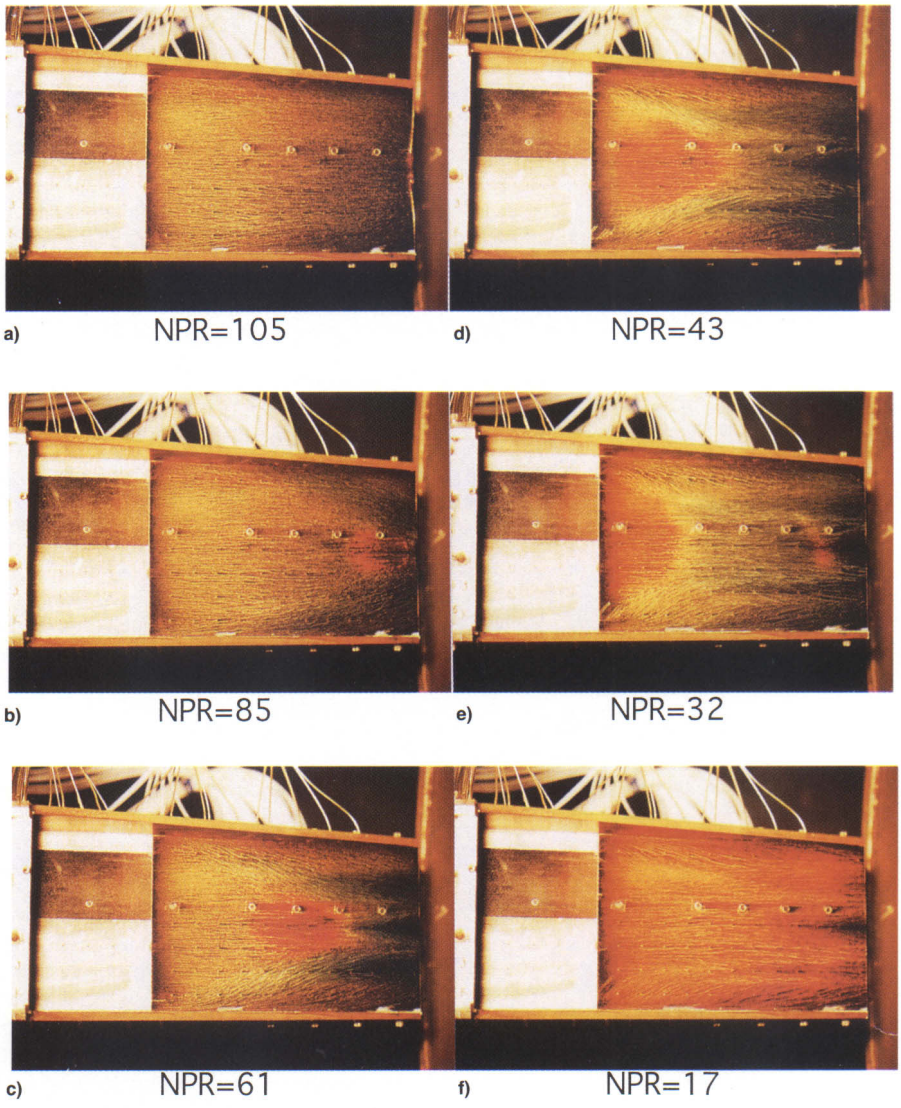

Fig. 5 Variation of shear stress distribution on ramp wall in overexpanded condition.

B. Characteristics of Flow on the Ramp

The investigation of flow characteristics on the ramp is important to understand the variation of the thrust coefficient in overexpanded condition. First, SSLC was used to visualize the shear stress distribution on the ramp. Figure 5 presents photographs taken at NPR = 105, 85, 61, 43, 32, and 17.

The flowfield shown in Fig. 5a is essentially the same as that in the underexpanded condition. When the flow is not affected by the ambient pressure, the color of SSLC is yellow-green, which shows that shear stress is strong. As NPR is decreased, a red region, whose shear stress is very weak, is observed in the vicinity of the center of the nozzle near the trailing edge Figs. 5b and 5c. The red region becomes larger and moves upstream as NPR is decreased. At NPR = 43 (Fig. 5d), the red region covers the whole span of the ramp. The upstream edge of the red region is straight and perpendicular to the X axis. When the flow on the ramp separates completely, SSLC turns red all over the ramp (Fig. 5f). The color of the red region in Fig. 5b is the same as in Fig. 5f. It is possible that the flow in the red region separates from the ramp.

The oil point method can indicate flow directions in the red region and all over the ramp. Figure 6 shows a comparison between a flow pattern produced by oil points and that produced by SSLC at NPR = 45. At the center of the ramp (X/Y^* = 100 to 115) in Fig. 6b, some of the points are directed to upstream of the ramp. These points correspond to the red region that shows weak shear stress. These results indicate that the red region is caused by flow separation and recirculation on part of the ramp.

The oil point method shows that the streamlines at X/Y^* = 75 near the side-fences suddenly turn toward the centerline of the ramp. This flow pattern, in which the streamlines converge to the center, is similar to that caused by a crossing shock wave/turbulent boundary-layer interaction in sidewall compression inlets.[12] Assuming the existence of a crossing shock wave in this nozzle flow, a pair of shock waves must be generated at the side-fences.

Figure 7 shows the pressure contours on the ramp measured at NPR = 3000, 90, and 45. Wall pressure is nondimensionalized by Pv in the respective conditions.

Figure 7a shows the pressure contour on the ramp of underexpanded EN5. Since the flow is not affected by Pv, it can be considered as a two-dimensional flow. The two peaks at X/Y^* = 45 and 83 are caused by the incidence of two compression waves generated by the GG nozzle contour.[8]

In contrast, Figs. 7b and 7c show the pressure contour in the overexpanded condition. The region affected by "back" pressure can be determined by these contours as the area where Ps/Pv becomes larger than that in Fig. 7a.

The contour at NPR = 90 in Fig. 7b shows that Ps near the side-fences at NPR = 90 begins to increase at X/Y^* = 90 and attains the ambient pressure at the trailing edge. At NPR = 45 (Fig. 7c), the wall pressure near the side-fences also increases to the ambient pressure at X/Y^* = 72. These

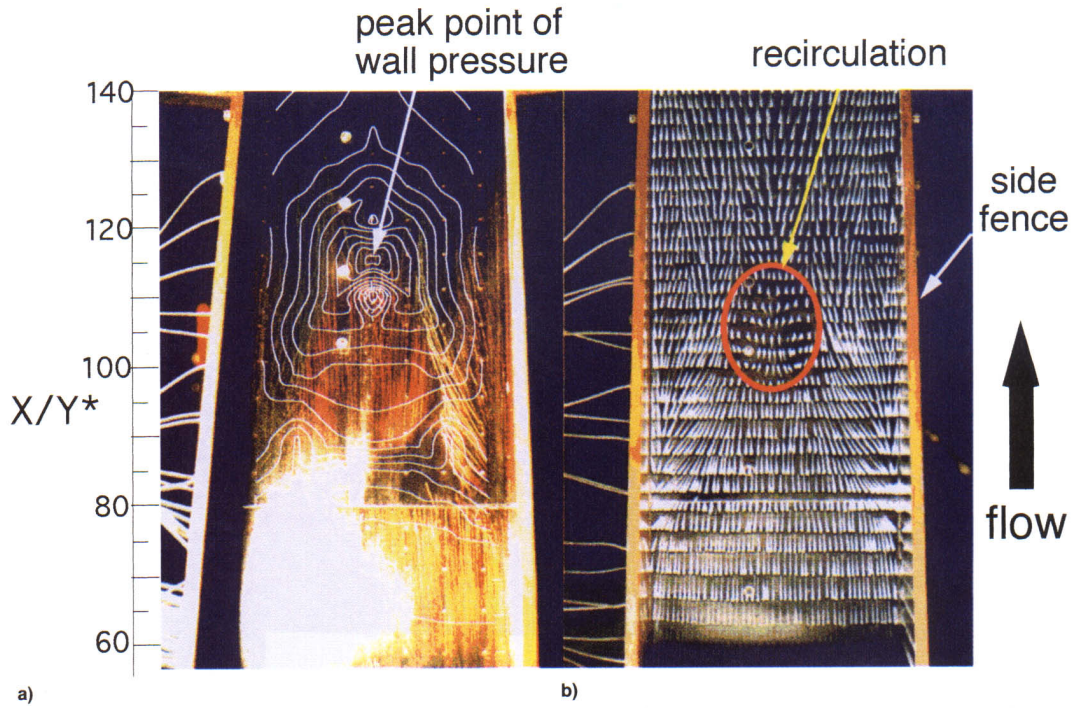

Fig. 6 Photographs of ramp wall at NPR = 45: a) shear stress distribution and wall pressure contour and b) flow directions.

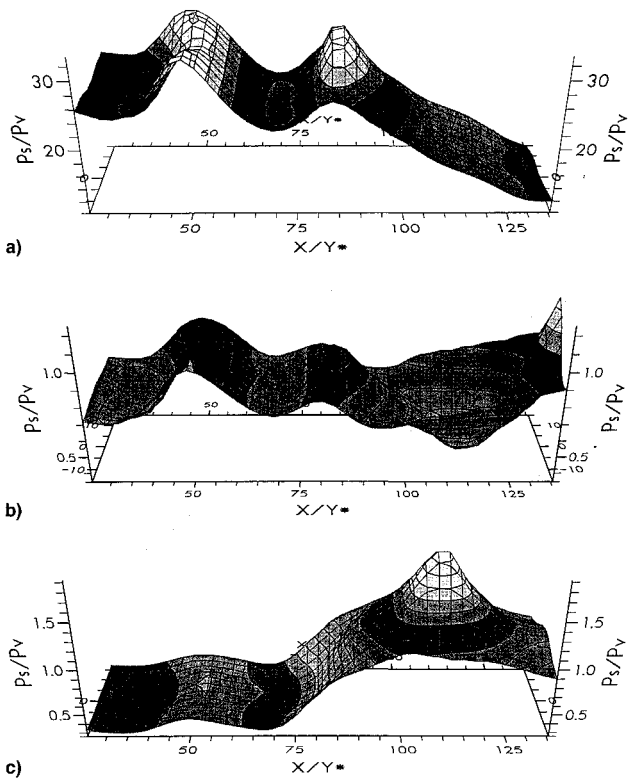

Fig. 7 Contours of ramp wall pressure nondimensionalized by *Pv*: a) at NPR = 3000 in underexpanded condition, b) at NPR = 90, and c) at NPR = 45 in overexpanded condition.

pressure distributions clearly show the presence of the separations on the side-fences. The peak pressure point at X/Y^* = 110 at NPR = 45 can be understood as being due to the crossing of a pair of shock waves from the side-fences. The pressure at that peak is about 9 times greater than *Ps* at X/Y^* = 70, which is not affected by *Pv*. The same value of the pressure rise in the inlet flow must be caused by the crossing shock waves generated at the edge of 11 deg.[12] Therefore, the flow on the side-fences is considered to separate without reattachment to the side-fences.

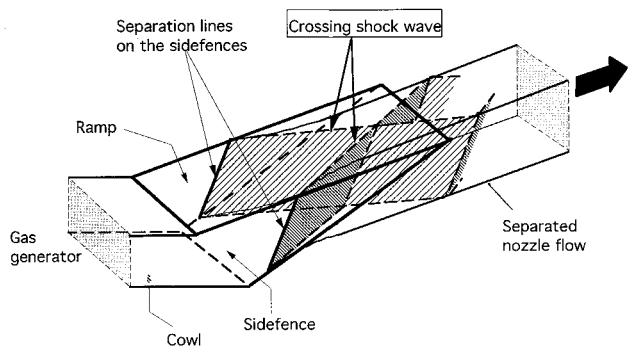

Fig. 8 Three-dimensional perspective view of the crossing shock waves in nozzle flow at NPR = 45 (separation bubble and its shock wave are omitted).

Figure 8 presents a schematic of the flowfield with the crossing shock wave in EN5 at NPR = 45. A pair of shock waves arise at the middle of the side-fences and cross at the center of the ramp. The exhaust flow in EN5 separates at the side-fences and the pressure adjustment to the *Pv* is made through the oblique shock waves. As NPR is decreased, the crossing shock wave/boundary-layer interaction becomes stronger as pressure must adjust to the higher *Pv* caused by the decrease of NPR. The low-shear stress region indicated by red in Fig. 6 corresponds to the pressure plateau at X/Y^* = 85 to X/Y^* = 110 in Fig. 7c. This plateau was caused by the strong interaction of the shock waves with the boundary layer on the ramp.[11] Therefore, the region whose boundary layer is affected by the interaction becomes larger and the front edge of separation moves upstream on the ramp faster than that on the side-fences. At NPR = 18, the separation edge reaches to the leading edge of the ramp. Then, the flow on the ramp separates completely without reattachment to the ramp.

The complicated variation of C_F in Fig. 4 can be understood if the three-dimensional flowfield mentioned above is taken into account. The regions where the wall pressure is higher than the ambient pressure in Fig. 6 yield positive performance, the values of which are ΔC_F = 2.5% at NPR = 90, and 4.5% at NPR = 45. These values make the experimental C_F greater than the prediction with the assumption of two-dimensional flow and separation.

These results for the rectangular, asymmetric nozzles depend on the aspect ratio of the nozzles. The separation vortices and the extent of the region influenced by the crossing shock wave are governed by the Reynolds number (the nozzle dimensions). In order to predict these phenomena, numerical calculations incorporating proper turbulent models are required. Results of three-dimensional Navier-Stokes computations were presented in a separate paper.[13]

IV. Conclusions

The variations of the thrust coefficients with NPR were measured in the scramjet nozzle to investigate the effect of the ambient pressure on the nozzle flow. The nozzle wall pressure was examined and the surface shear stress and flow directions were visualized. Comparisons between these measurements lead to the following conclusions:

1) The thrust coefficients of the underexpanded EN5 can be predicted using the assumption of two-dimensional nozzle flow. In contrast, the C_F in the overexpanded condition does not agree with the prediction. The C_F at NPR $<$ 100 varied from 97.8 to 85% from the optimum NPR = 284 to NPR = 18 in a complicated manner.

2) The shear stress distributions and the oil points in the overexpansion flow clarified a three-dimensional flow on the ramp that is analogous to a sidewall compression inlet flow. The flowfield in the overexpanded EN5 is characterized with the crossing shock wave and its interaction with the turbulent boundary layer on the ramp. The interaction creates a separation region at the center of the ramp that moves upstream and becomes larger as NPR is decreased.

3) The crossing shock wave and the interaction produce regions where the pressure on the ramp is greater than the ambient pressure. The point of the peak pressure moves upstream as NPR is decreased and separation on the side-fences moves upstream. The positive thrust at the regions complicates the variation of the thrust coefficient and results in nozzle performance superior to the predicted performance.

Acknowledgments

This study was conducted as a joint research project with Ishikawajima–Harima Heavy Industries, Co., Ltd. The authors are grateful to many researchers for their assistance.

References

[1]Dusa, D. J., "Turboramjet Exhaust Nozzle System," *Proceedings of the 10th International Symposium on Air Breathing Engines*, AIAA, Washington, DC, 1991, pp. 1100–1110 (ISABE Paper 91-7118).

[2]Snyder, D. D., and Pinckney, S. Z., "A Configuration Development Strategy for the NASP," *Proceedings of the 10th International Symposium on Air Breathing Engines*, 1991 (ISABE Paper 91-7056).

[3]Wasko, R. A., "Performance of Annular Plug and Expansion-Deflection Nozzles Including External Flow Effects at Transonic Mach Numbers," NASA TND-4462, April 1968.

[4]Ruffin, S. M., "Hypersonic Single Expansion Ramp Nozzle Simulations," *Journal of Spacecraft and Rockets*, Vol. 29, Nov.–Dec. 1992, pp. 749–755.

[5]Watanabe, S., "A Scramjet Nozzle Experiment with Hypersonic External Flow," AIAA Paper 92-3289, July 1992.

[6]Zeutzius, M., and Beylich, A. E., "Experimental Investigation of Asymmetric Nozzles for Advanced Hypersonic Space Planes—Structure of Nozzle Jets and Thrust Vector Control," *Zeitschrift Flugwissenschaften und Weltraumforschung*, Vol. 17, No. 5, 1993, pp. 311–322.

[7]Nickerson, G. R., "Optimized Supersonic Exhaust Nozzles for Hypersonic Propulsion," AIAA Paper 88-3161, 1988.

[8]Mitani, T., Ueda, S., Tani, K., Sato, S., Miyajima, H., Matsumoto, M., and Yasu, S., "Validation Studies of Scramjet Nozzle Performance," *Journal of Propulsion and Power*, Vol. 9, No. 5, 1993, pp. 725–730.

[9]Flugstad, T. H., Romine, B. M., and Whittaker, R. W., "High Mach Exhaust System Concept Scale Model Test Results," AIAA Paper 90-1905, July 1990.

[10]Mikkelsen, K. L., and Idzrek, J. J., "Experience in the Operation of a Hypersonic Nozzle Static Thrust Stand," AIAA Paper 92-3292, July 1992.

[11]Arens, M., and Spiegler, E., "Shock-Induced Boundary Layer Separation in Overexpanded Conical Exhaust Nozzles," *AIAA Journal*, Vol. 1, No. 3, 1963, pp. 578–581.

[12]Garrison, T. J., and Settles, G. S., "Interaction Strength and Model Geometry Effects on the Structure of Crossing-Shock Wave/Turbulent Boundary Layer Interactions," AIAA Paper 93-0780, Jan. 1993.

[13]Ishiguro, T., Takaki, R., Hiraiwa, T., and Mitani, T., "A Three-Dimensional Analysis of Scramjet Nozzle Flows," AIAA Paper 93-5059, Dec. 1993.